JOURNAL OF GEOPHYSICAL RESEARCH, VOL. 113, B05410, doi:10.1029/2007JB005291, 2008

Impact of bending related faulting on the seismic properties of the incoming oceanic plate offshore of Nicaragua

Monika Ivandic,[1] Ingo Grevemeyer,[2] Arnim Berhorst,[2] Ernst R. Flueh,[2] and Kirk McIntosh[3]

Received 23 July 2007; revised 17 December 2007; accepted 30 January 2008; published 30 May 2008.

[1] A seismic wide-angle and refraction experiment was conducted offshore of Nicaragua in the Middle American Trench to investigate the impact of bending-related normal faulting on the seismic properties of the oceanic lithosphere prior to subduction. On the basis of the reflectivity pattern of multichannel seismic reflection (MCS) data it has been suggested that bending-related faulting facilitates hydration and serpentinization of the incoming oceanic lithosphere. Seismic wide-angle and refraction data were collected along a transect which extends from the outer rise region not yet affected by subduction into the trench northwest of the Nicoya Peninsula, where multibeam bathymetric data show prominent normal faults on the seaward trench slope. A tomographic joint inversion of seismic refraction and wide-angle reflection data yield anomalously low seismic *P* wave velocities in the crust and uppermost mantle seaward of the trench axis. Crustal velocities are reduced by 0.2–0.5 km s^{-1} compared to normal mature oceanic crust. Seismic velocities of the uppermost mantle are 7.6–7.8 km s^{-1} and hence 5–7% lower than the typical velocity of mantle peridotite. These systematic changes in *P* wave velocity from the outer rise toward the trench axis indicate an evolutionary process in the subducting slab consistent with percolation of seawater through the faulted and fractured lithosphere and serpentinization of mantle peridotites. If hydration is indeed affecting the seismic properties of the mantle, serpentinization might be reaching 12–17% in the uppermost 3–4 km of the mantle, depending on the unknown degree of fracturing and its impact on the elastic properties of the subducting lithosphere.

Citation: Ivandic, M., I. Grevemeyer, A. Berhorst, E. R. Flueh, and K. McIntosh (2008), Impact of bending related faulting on the seismic properties of the incoming oceanic plate offshore of Nicaragua, *J. Geophys. Res.*, *113*, B05410, doi:10.1029/2007JB005291.

1. Introduction

[2] The understanding of the Earth's water cycle is inherently linked to the subduction of water at subducting plate boundaries. The transfer of water into the deep Earth's interior is related to the alteration and hydration of the incoming lithosphere. The release of water from subducting lithospheres affects the composition of the mantle wedge, enhances partial melting and triggers intermediate-depth earthquakes. Water is transferred with the incoming plate into the subduction zone as water trapped in sediments and void spaces in the igneous crust and as chemically bound water in hydrous minerals in sediments and oceanic crust [e.g., *Staudigel et al.*, 1996; *Jarrad*, 2003]. However, if water reaches upper mantle rocks prior to subduction, significant amounts can be transferred into the deep subduction zone as water-bearing mineral serpentine [*Phipps Morgan*, 2001; *Peacock*, 2001, 2004]. Serpentinites have nearly the same chemical composition as mantle peridotite except that they contain approximately 13 wt % water in mineral structures and are less dense.

[3] The mechanism by which dehydration reactions trigger intermediate-depth earthquakes is based upon a pore pressure increase that reduces effective normal stress and hence can promote seismic rupture [*Raleigh and Paterson*, 1965; *Meade and Jeanloz*, 1991]. Serpentinized mantle generally dehydrates at higher temperature and pressure than sediment and hydrothermally altered crust. The most stable serpentine mineral antigorite dewaters progressively down to approximately 200 km depth, suggesting that serpentines may be the primary agent to deliver water into the mantle.

[4] Outer rise earthquakes have been attributed to plate bending tensional stresses [*Chapple and Forsyth*, 1979]. The bending of the plate is associated with tension in the upper ~20 km [*Christensen and Ruff*, 1983; *Lefeldt and Grevemeyer*, 2008]. Bathymetric observations of abundant faults on the seaward side of the trench axis [e.g., *Masson*, 1991; *Dmowska et al.*, 1996; *Kobayashi et al.*, 1998]

[1] Sonderforschungsbereicht 574, Kiel, Germany.
[2] Leibniz Institut fuer Meereswissenschaften, IFM-GEOMAR, Kiel, Germany.
[3] Institute for Geophysics, University of Texas at Austin, Austin, Texas, USA.

0148-0227/08/2007JB005291$09.00

suggest that plate bending and normal faulting are inherently related. In addition, multichannel seismic reflection (MCS) data indicate that a number of these faults cut through the crust into the uppermost mantle [*Ranero et al.*, 2003; *Grevemeyer et al.*, 2005]. Large amounts of seawater may percolate through these faults into the oceanic lithosphere and change its chemical composition and mechanical and seismic properties. It has been suggested that most of the hydration by this mechanism occurs at the outer rise [e.g., *Ranero et al.*, 2003; *Peacock*, 2001, 2004], where seismological studies suggest that faults cut >20 km into the lithosphere [*Kanamori*, 1971; *Christensen and Ruff*, 1988; *Hasegawa et al.*, 1994; *Lefeldt and Grevemeyer*, 2008], providing potential pathways for seawater to infiltrate and react with the underlying mantle. However, so far evidence from seismic studies for an impact of serpentinization on the seismic properties has only been found within tectonically dominated ultraslow spreading crust [*Osler and Louden*, 1995; *Grevemeyer et al.*, 1997]. However, seismic wide-angle and refraction data recently collected offshore Nicaragua [*Grevemeyer et al.*, 2007], where *Ranero et al.* [2003] imaged faults that cut up to 20 km into the mantle suggest that seismic velocity in the uppermost mantle are anomalously low (<7.7 km s^{-1}). Existing data sets, however, cover only the area trenchward of the outer rise bulge and hence fail to show that crust cutting faults and low mantle velocities are related to an evolutionary process caused by bending-related faulting as the plate approaches the deep sea trench. Thus, the observed features may have been inherited at the spreading center.

[5] In order to determine whether low velocities in the mantle are indeed caused by processes related to the plate bending and faulting prior to subduction, additional data were collected offshore of Nicaragua aboard of the German research vessel *Sonne.* Our profile P50 extends from the trench axis into the area seaward of the outer rise, where the lithosphere is still not affected by bending-related stresses and hence faulting. Results of this experiment presented here document that the crust and upper mantle rocks of the subducting Cocos plate, formed ~24 Ma ago at the fast spreading East Pacific Rise, undergo an extensive alteration (perhaps hydration) prior to subduction due to plate bending and plate faulting.

2. Tectonic Settings

[6] The study area is located offshore of Nicaragua seaward of the Middle American Trench, where the Cocos plate, formed at the fast spreading East Pacific Rise to the west and the Cocos Nazca Spreading Center to the south, subducts beneath the Caribbean plate, dragging down crustal material and sediments (Figure 1). Off Nicaragua, the Cocos slab subducts with a rate of about 91 mm a^{-1} [*DeMets et al.*, 1990] in a northeasterly direction. The dip of the Benioff zone, obtained from teleseismic [*Burbach et al.*, 1984] and local network [*Protti et al.*, 1994] seismic data, ranges from 25° in the seismogenic zone to 84° between 100 and 220 km depth. Before entering the trench, the incoming plate, which was formed roughly 24 Ma ago at the East Pacific Rise, is pervasively normal faulted with offsets of up to 100–500 m and length of 10–50 km [*von Huene et al.*, 2000; *Ranero et al.*, 2003]. Offshore of Nicaragua, faulting and fault growth between the outer rise and the trench generate a prominent stair-like seafloor relief prior to subduction (Figure 1). Normal faults are poorly developed or absent seaward of the outer bulge apparently forming as the plate approaches the trench. The area of normal faulting on the subducting plate off Nicaragua shows a system of half grabens bordered by faults parallel to the trench, progressing downward into the trench as the Cocos plate subducts. Deep-tow video observations show that normal faults often expose basement; heat flow data suggest that these exposed faults govern a hydrothermal circulation system in the incoming plate [*Grevemeyer et al.*, 2005]. In addition, seamounts off Nicoya Peninsula seem to control the thermal state of the incoming plate and mine heat from the Cocos plate [*Fisher et al.*, 2003]. Multichannel seismic reflection (MCS) data acquired offshore of Nicaragua [*Ranero et al.*, 2003] suggest that some normal faults may cut through the entire crust of the incoming plate, reaching several kilometers into the upper mantle and hence may facilitate migration of seawater down to the upper mantle.

3. Data and Methodology

[7] The data used in this study consist of ocean bottom hydrophone data from a wide-angle profile acquired in 2003 aboard the German R/V *Sonne* (Figure 1). The working area of the cruise was located at the Pacific continental margin off Costa Rica and Nicaragua. The profile P50 was shot with three 32 Liter BOLT Inc. air guns, providing a total volume of 96 L, and the air guns were operated at a pressure of 150 bar. A shot interval of 60 s and a speed of 3.5 knots gave an average shot spacing of 100 m. The seismic data were recorded by 12 ocean bottom hydrophones (OBH) [*Flueh and Bialas*, 1996] and 5 ocean bottom seismometers (OBS) [*Bialas and Flueh*, 1999]. P50 is 140 km long and extends from seaward of the outer rise into the trench northwest of the Nicoya Peninsula. This location was chosen because it covers the area of significant bending and as a consequence normal faults are abundant in swath mapping bathymetric data [e.g., *Ranero et al.*, 2003]. In addition, a major portion of the profile is coincident with the MCS line NIC20 (Figure 2a) shot in the year 2000 with the multichannel seismic equipment of Lamont-Doherty Earth Observatory's seismic vessel *Maurice Ewing*. The seismic MCS data imaged the sedimentary blanket and oceanic crust, including a prominent Moho reflection at ~1.8 s below basement (Figure 2b). Unfortunately, the rough seafloor and basement topography scatters seismic energy where plate bending and normal faulting is most prominent [*Berhorst*, 2006]. Therefore, Moho and faults cutting through the crust into the mantle could not be imaged within ~20 km of the trench axis. In addition, NIC20 provides seismic refraction data from the trench and the continental slope. Three stations from NIC20 (OBH01, OBH02 and OBH03) in the trench and on the lower continental slope were included into the data inversion procedure. The record sections obtained at selected OBHs are shown in Figure 3.

[8] Most refraction surveys with this objective are interpreted relative to the average structure of oceanic crust as defined by *White et al.* [1992]. However, it is known that

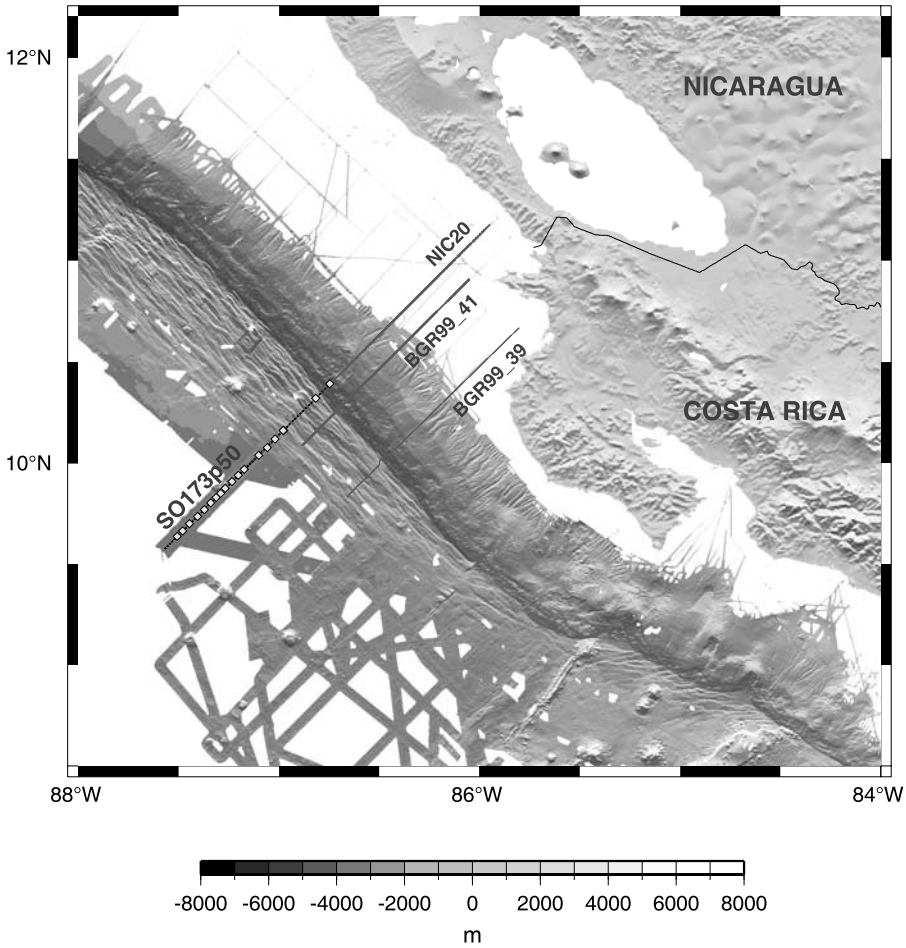

Figure 1. Bathymetric-topographic map of the Central American subduction zone offshore of Costa Rica and Nicaragua. The working area of the cruise SO173-1 with the wide-angle and refraction profile p50 is located northwest of the Nicoya Peninsula. Squares indicate ocean bottom stations used in the seismic modeling. Three stations from the line NIC20 in the trench and on the lower continental slope were included in the data inversion procedure. Along MCS profiles BGR99_41 and BGR99_39, *Ranero et al.* [2003] imaged trenchward dipping reflectors, interpreted as faults cutting through the crust into the mantle.

the oceanic crust in the east Pacific Ocean is generally much thinner than the 6.48 ± 0.75 km thickness given by *White et al.* [1992] for crust younger than 30 Ma [e.g., *Collins et al.*, 1989; *Grevemeyer et al.*, 1998; *Walther et al.*, 2000]. Therefore, we based our one-dimensional reference velocity model on the structure of crust studied during the presite survey work of Ocean Drilling Program (ODP) Leg 206 in the Guatemala Basin westward of Nicaragua [*Wilson et al.*, 2003]. In this one-dimensional model, upper crustal velocities are 4.5–5 km s^{-1}. The transition to lower crust is at ~1.5 km below the basement. Lower crustal velocities are between 6.8 and 7.1 km s^{-1}. Total crustal thickness is ~5–5.5 km. Upper mantle peridotite velocity is 8.2 km s^{-1}.

[9] A two-dimensional velocity model along the profile was calculated using the joint refraction and reflection inversion of *Korenaga et al.* [2000], which solves for the seismic velocity field and the depth of a reflecting interface. The forward problem is solved by a hybrid method based on shortest path [e.g., *Moser*, 1991] and ray-bending [e.g., *Moser et al.*, 1992] methods, and the inverse problem uses a sparse least squares method [*Paige and Saunders*, 1982] to solve a regularized linear system. We applied this method in a layer-stripping approach, where the appropriate phases are used to constrain the shallow structure first and then to progressively constrain the deeper layers. A total of 3596 *Pg*, 1894 *PmP* and 1747 *Pn* phases were hand-picked from 19 instruments (16 P50, 3 NIC20). A low ambient noise level and the good quality of waveforms made picking of the first breaks relatively straightforward. Upper crustal arrivals could be picked to ±12 ms, or better. However, for larger offsets signal-to-noise ratio decreases. Uncertainties as large as ±90 ms have been assigned to some *Pn* and *PmP* arrivals.

[10] The two-dimensional velocity field is parameterized by a grid of nodes hanging from the seafloor topography with 0.5 km lateral nodal spacing and variable vertical nodal (0.05 km within the upper 2 km and increasing to 0.4 km at the bottom). The Moho is parameterized as a floating reflector with nodes every 1 km with one degree of freedom in the vertical direction. We applied smoothing constraints

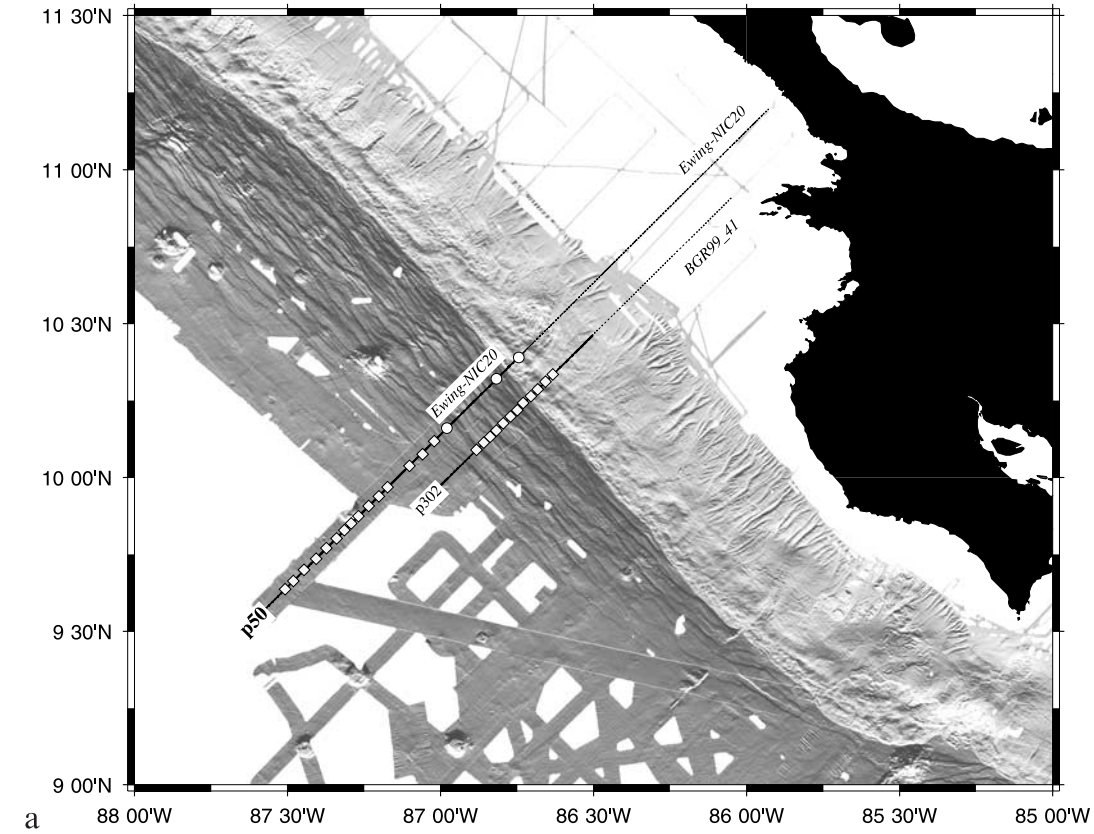

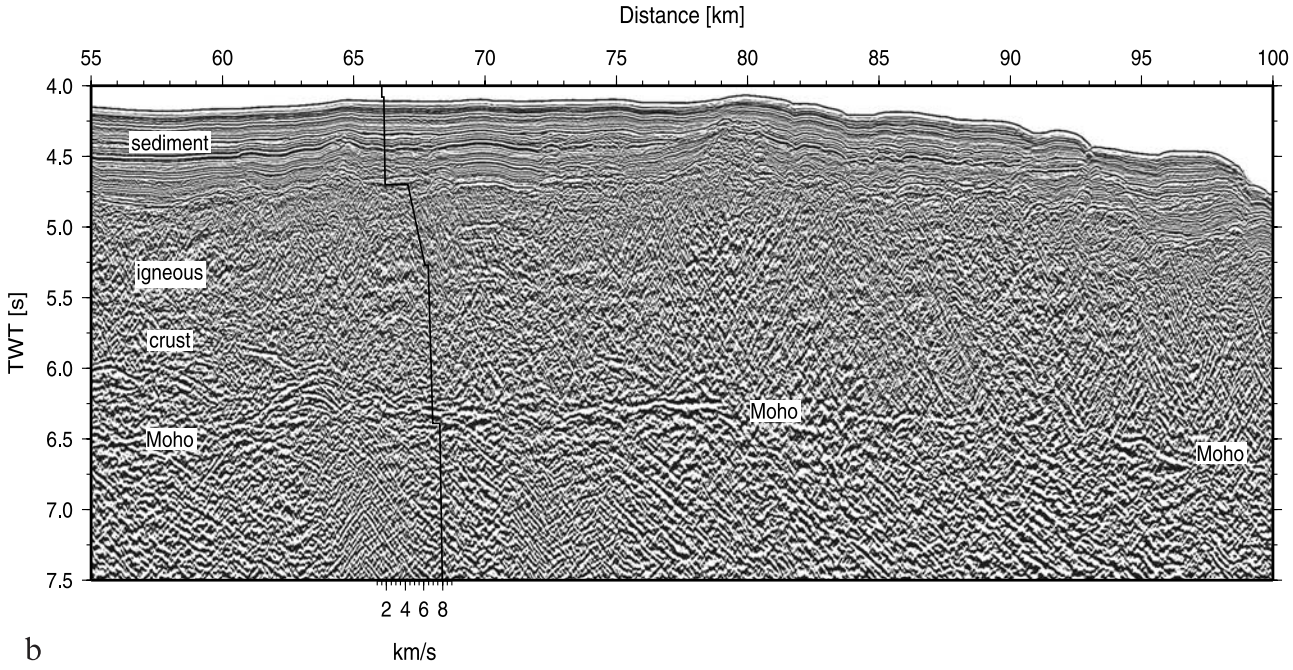

Figure 2. (a) Multibeam bathymetric map of the Cocos plate and continental slope offshore of Costa Rica and Nicaragua. A major portion of the profile p50 is coincident with the MCS line NIC20. Seismic line p302 from *Grevemeyer et al.* [2007] acquired during R/V *Sonne* cruise SO173-1 covers only the area trenchward of the outer rise bulge. (b) Seismic data from the MCS line NIC20 imaged the sedimentary blanket and oceanic crust, including a prominent Moho reflection at ~1.8 s below the basement. The one-dimensional velocity profile is a time-converted velocity-depth profile from the modeling approach, showing an excellent fit between MCS and seismic refraction and wide-angle data. The distance scale coincides with the one in the seismic refraction line.

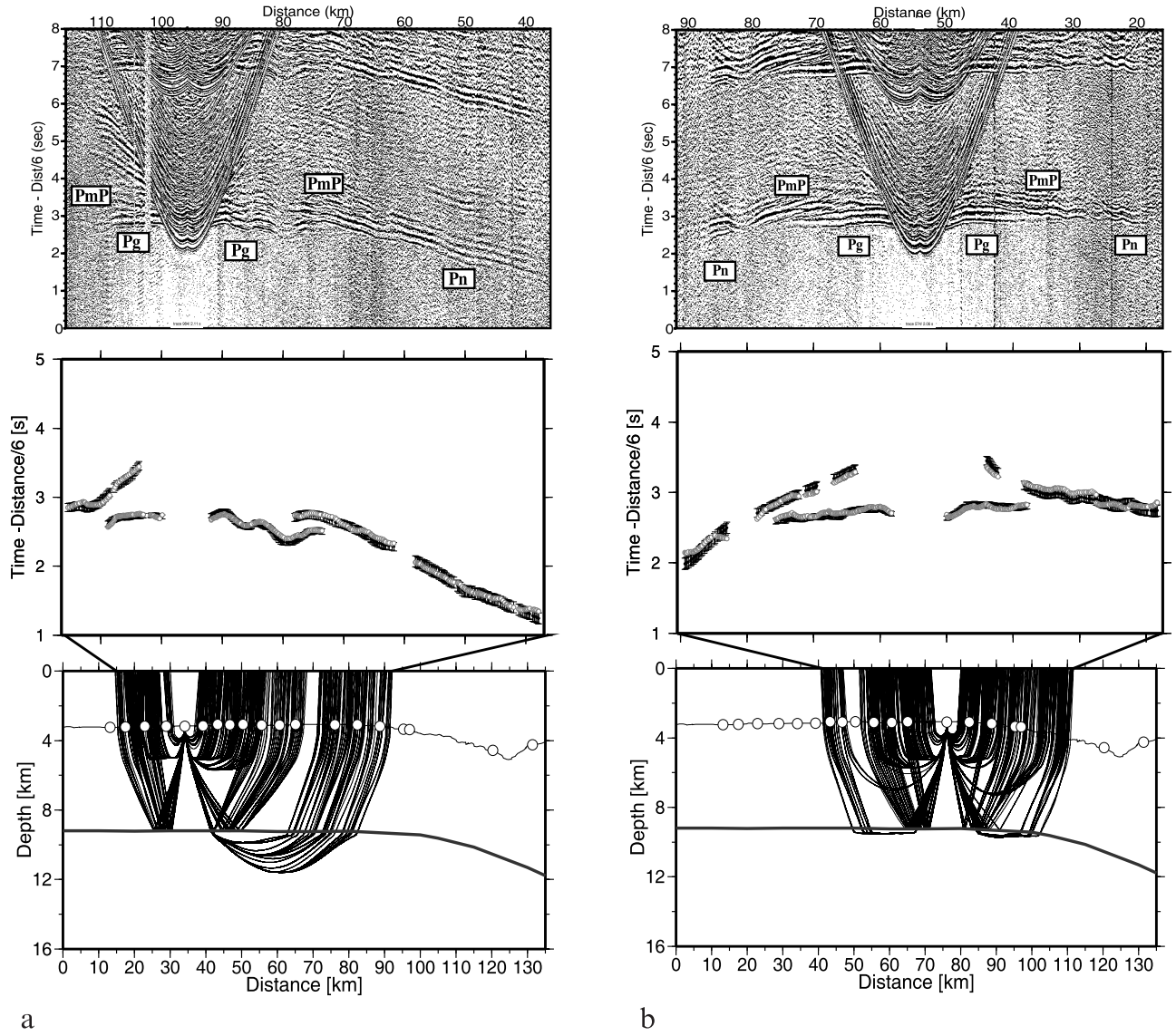

Figure 3. (top) Wide-angle data examples from selected instruments. Data have been reduced at 6 km s^{-1}. (middle) Picked travel times (solid circles with error bars) and predicted travel times (white circles) for *Pg*, *PmP* and *Pn* phases. (bottom) Plots of the corresponding raypaths. (a) OBH38, (b) OBH47, (c) OBH 01, and (d) OBH03.

on both velocity and depth perturbations using predefined correlation lengths in order to stabilize the inversion. In addition, damping constraints for velocity and depth are added to the regularized linear system. A detailed description of the method and parameters is given elsewhere [*Korenaga et al.*, 2000]. The model is 135 km long and 20 km deep. For the horizontal correlation lengths we used values varying from 4 at the top to 10 at the bottom, and vertical correlation lengths vary from 0.1 km at the top to 3 km at the bottom. Also, the depth sensitivity is weighted by a depth kernel weighting parameter (w). For the inversion of *Pg* and *PmP* phases we used $w = 1$, which allows the same perturbations for both velocity and depth, and for the final inversion step, where all the phases were included, this parameter had a value of 0.1, allowing more perturbations for the velocity than for the depth. The RMS travel time misfit obtained for the final model is 50 ms [$\chi^2 = 0.99$], significantly reducing the initial misfit of 143 ms.

4. Seismic Structure

[11] The structure of the subducting oceanic lithosphere is resolved by intracrustal refractions (*Pg*), Moho reflections (*PmP*), and upper mantle refractions (*Pn*). The resultant two-dimensional velocity model (Figure 4a) reveals systematic changes in seismic properties of the lithosphere affected by plate flexure and faulting. No refracted phase from the sediment is observed, but seismic reflection data from NIC20 provide information on sediment thickness. The thin sediment cover has an average thickness of approximately 500 m with velocities ranging from 1.7 up to 1.8–1.85 km s^{-1}. The oceanic crust is typically divided

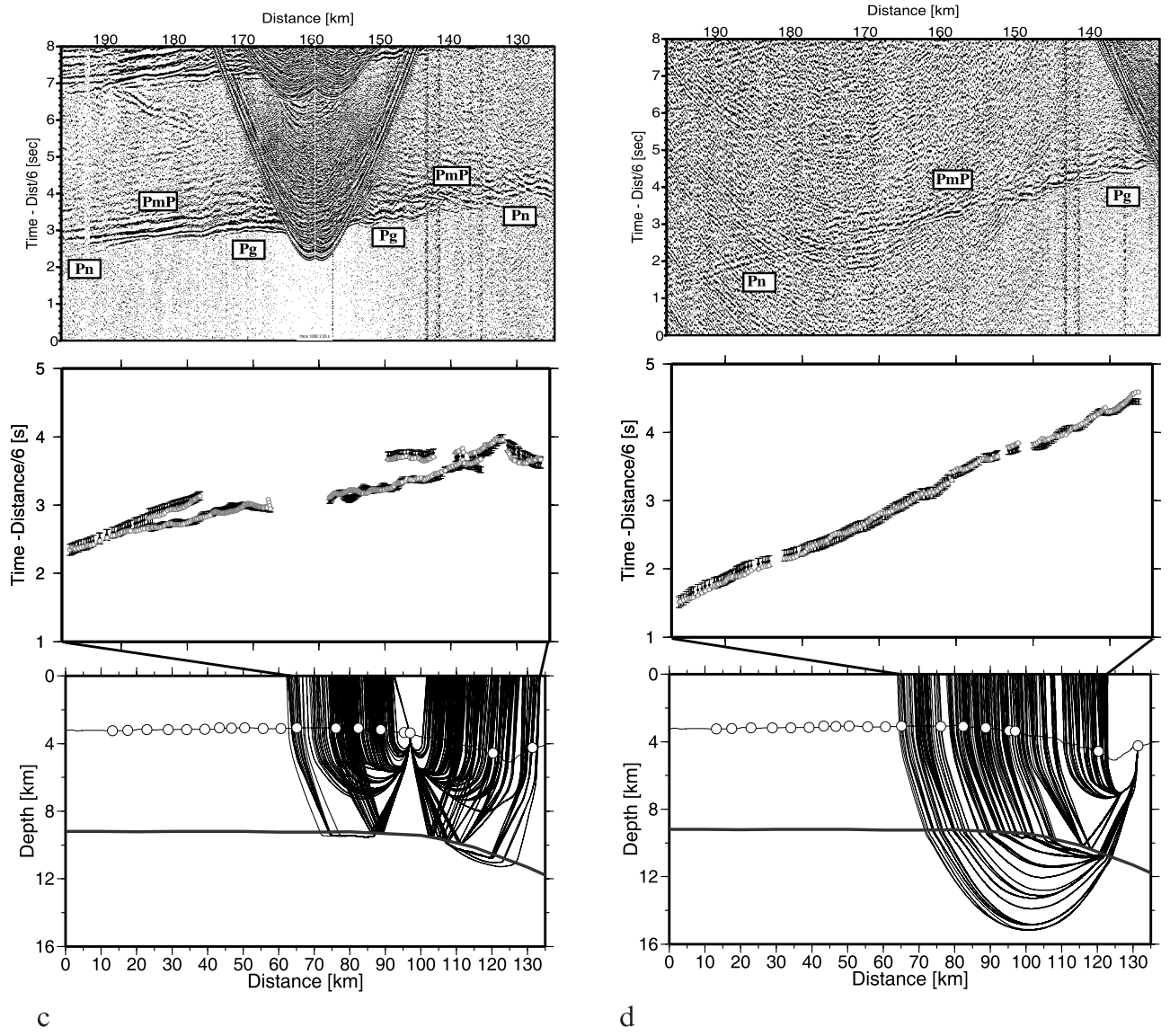

Figure 3. (continued)

into two primary layers: an upper crust (layer 2) characterized by a rapid increase in seismic velocity with depth ($\sim$1 km s^{-1} km^{-1}), and a thicker lower crust (layer 3) which is distinguished from layer 2 by both a higher *P* wave velocity and a much smaller vertical velocity gradient (0.1–0.2 km s^{-1} km^{-1}). In the outer rise region no significant lateral changes are found within the crust and uppermost mantle. Upper crustal velocities increase from 4.4 to 4.5 km s^{-1} at the top of the basement to 6.0–6.2 km s^{-1} at the bottom of layer 2, which is found at a depth of $\sim$1.5 km below the basement uniformly along the whole profile. These velocities have been commonly attributed to normal mature oceanic upper crust [*Grevemeyer et al.*, 1998, 1999; *Carlson*, 1998] and would correspond to a layer mainly composed of extrusive basalts and underlying sheeted dikes. Lower crustal velocities increase steadily from 6.5 to 6.7 km s^{-1} at the top to 7.0–7.1 km s^{-1} at the crust-mantle boundary, suggesting a crust of gabbroic composition [e.g., *White et al.*, 1992]. Strong wide-angle reflections from the Moho indicate a uniform crustal thickness of $\sim$5.5 km along the profile, confirming the results from the MCS survey. Below the Moho, in the uppermost mantle, we find a typical velocity of unaltered olivine-rich peridotites of 8.1–8.2 km s^{-1}.

[12] Toward the trench, however, crustal and upper mantle velocities are reduced compared to velocities expected for $\sim$24 Ma old mature oceanic lithosphere [e.g., *White et al.*, 1992; *Carlson*, 1998; *Grevemeyer and Bartetzko*, 2004], indicating a change in rock properties. Figure 4b shows the velocity reduction found in the subducting crust and upper mantle. Upper crustal velocities in layer 2 decrease to 4.1–4.3 km s^{-1} at the top and <6 km s^{-1} at the base. In the near-trench region velocities of the lower crustal rocks are reduced to 6.2–6.4 km s^{-1} at the top to $\sim$6.6–6.9 km s^{-1} and the bottom of layer 3. Two possible mechanisms may explain the observations: (1) fracture

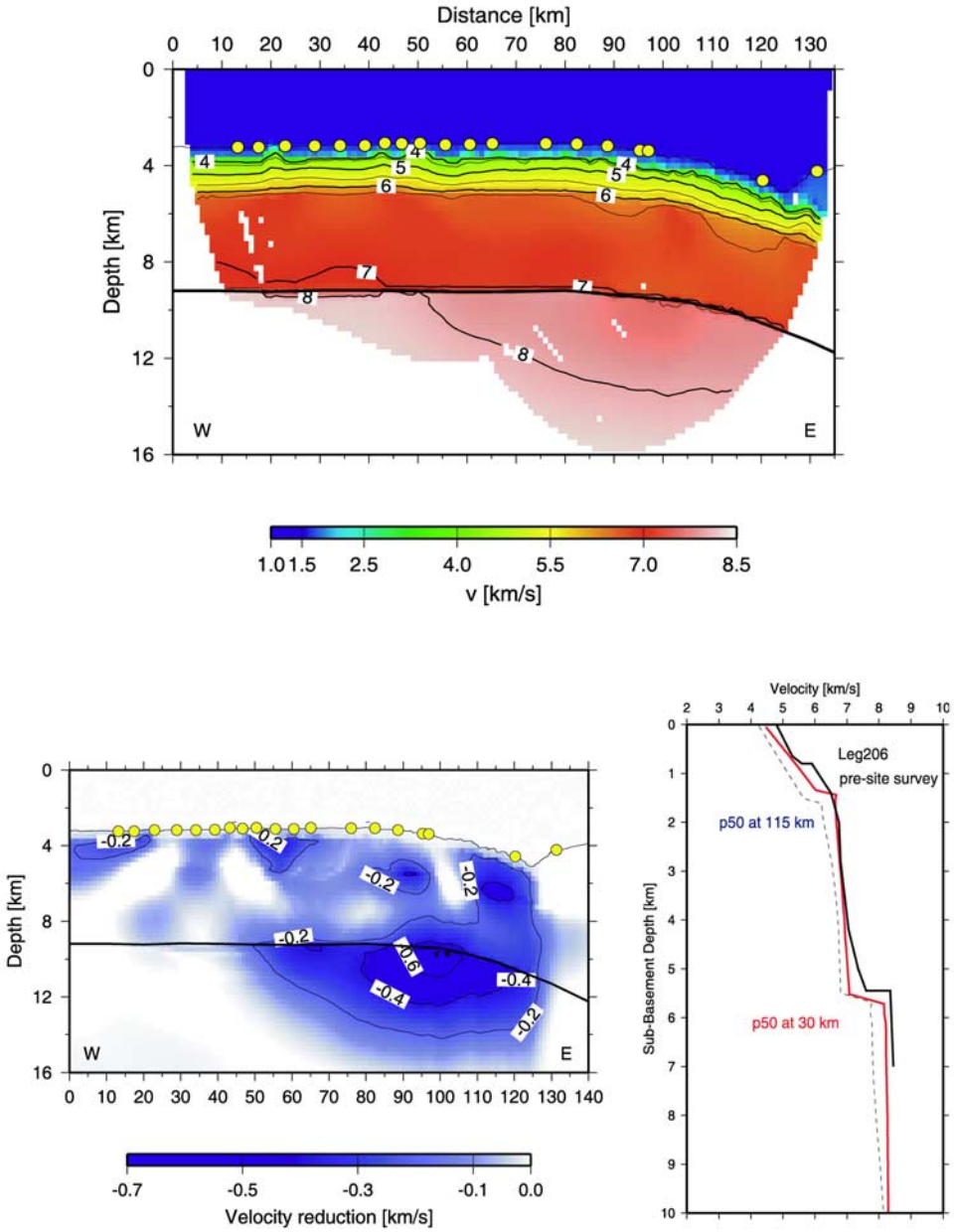

Figure 4. Result of tomographic inversion along profile p50 (Figure 1) using *Pg*, *PmP*, and *Pn* phases. (a) Final velocity model with isovelocity contours. Thick black line represents Moho boundary derived from inversion of *PmP* phases. Yellow circles indicate OBH and OBS stations. (b) Velocity anomalies in the crust and upper mantle. (c) Comparison of seismic velocity-depth profiles at two selected locations in the outer rise and near-trench region with 1-D reference velocity model from the presite survey work of Ocean Drilling Program Leg 206 in the Guatemala Basin westward of Nicaragua.

porosity has been increased, and/or (2) crustal rocks have been hydrated. However, the most prominent feature of the seismic velocity model is an extensive zone of reduced velocity in the uppermost mantle in the near-trench region. Changes in seismic structure start at ~60 km distance from the trench; the anomaly reaches its largest amplitude and extent near the trench axis. The velocity just below the Moho boundary is reduced to 7.6–7.8 km s^{-1}, what is 5–7% lower than the ~8.1–8.2 km s^{-1} found seaward of the outer rise region, perhaps indicating partially hydrated mantle associated with bending-related faulting [*Grevemeyer et al.*, 2007]. Figure 4c shows velocity-depth profiles extracted at selected locations in the outer-rise and near-trench region, indicating a change in the seismic structure as the plate approaches the trench.

5. Resolution and Sensitivity Test

[13] The derivative weight sum (DWS) value is a measure of the ray density near a grid point [*Toomey and Foulger*,

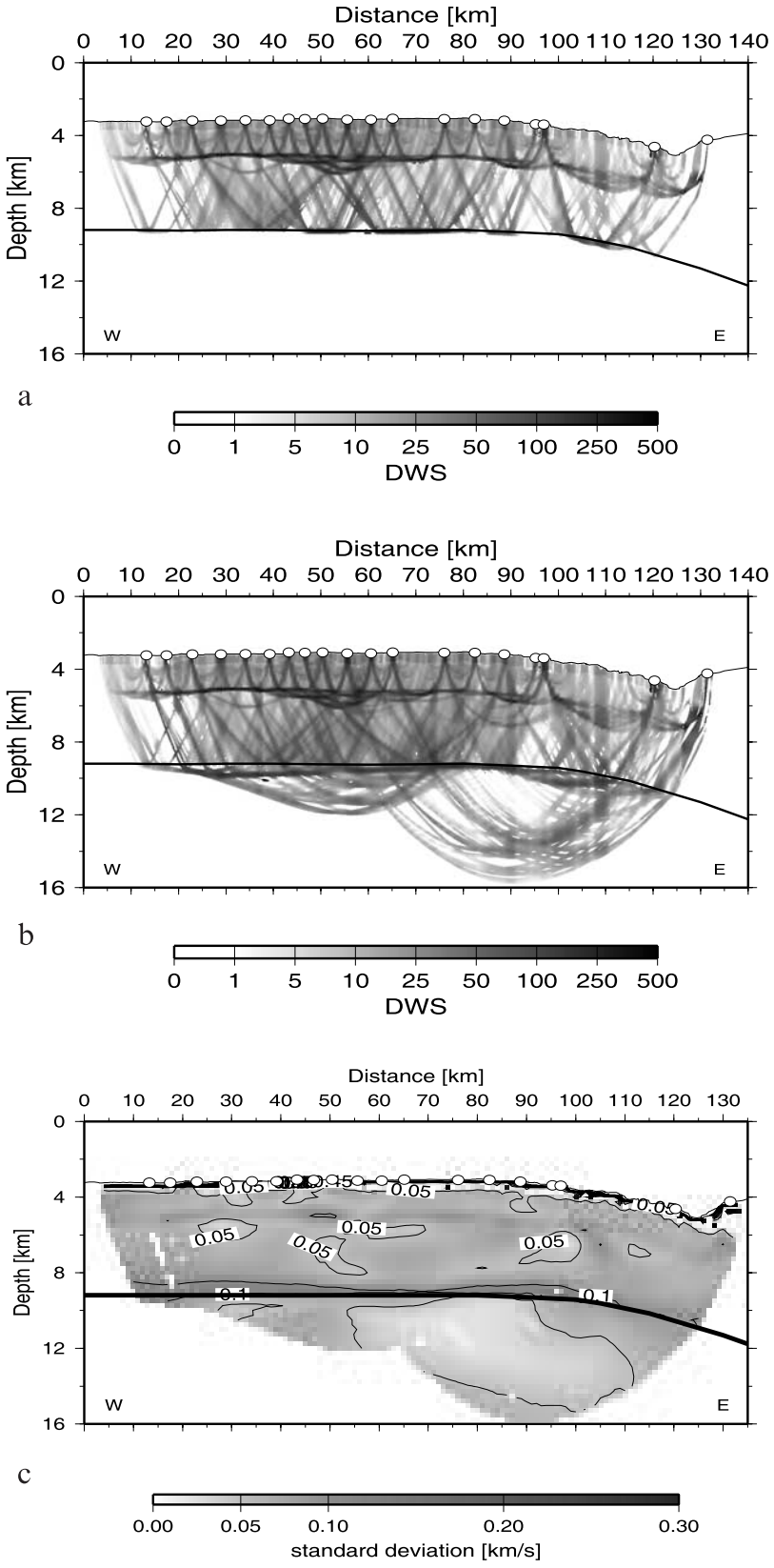

Figure 5. (a) Derivative weight sum (DWS) for crustal and *PmP* phases showing that the MCS data (Figure 2b) provide good constraints on the Moho depth. (b) Distribution of DWS values for the final velocity model shown in Figure 4a. (c) Velocity uncertainties derived from the Monte Carlo analysis.

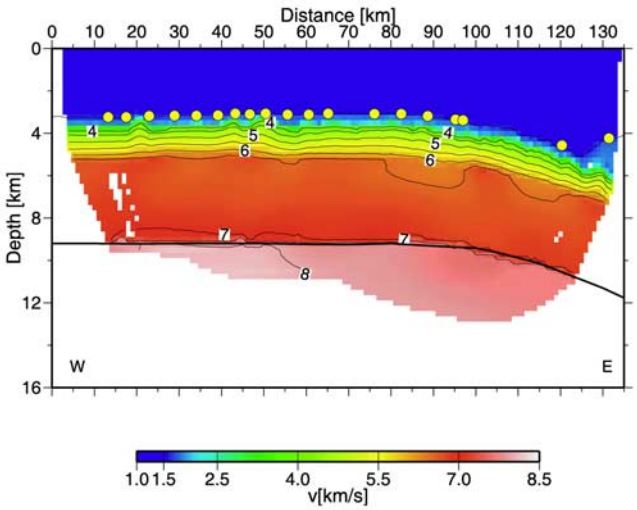

Figure 6. Result of tomographic inversion along profile p50 using a starting model with velocities well reduced compared to the first starting model.

1989]. The DWS for crustal phases (Figure 5a) indicates that the MCS data (Figure 2b) provide good constraints on the Moho depth. Figure 5b shows the DWS for all the phases used to construct the final velocity model.

[14] In order to estimate the uncertainties of the final model we applied Monte Carlo analysis [e.g., *Korenaga et al.*, 2000]. The uncertainty of a nonlinear inversion can be expressed in terms of the posterior model covariance matrix [e.g., *Tarantola*, 1987], which can be approximated by the standard deviation of a large number of Monte Carlo realizations assuming that all the realizations have the same probability [e.g., *Tarantola*, 1987]. A set of 10 initial models is constructed by randomly perturbing the velocity of the crustal and upper mantle nodes (±0.3 km s^{-1}) of our reference model. We also generated 10 different data sets by adding random phase gradient errors (±0.50 ms) and common receiver noise (±0.30 ms) to the initial data set [*Zhang and Toksöz*, 1998]. We obtained 100 Monte Carlo realizations by inverting all the combinations of the 10 initial velocity models with the 10 observation vectors, using the same model parameterization as in the final solution. All of the Monte Carlo inversions converged in less then 6 iterations to $\chi^2 \sim 1$, where the model error is equal to the data uncertainty. The standard deviation of the velocity is found to be lower than 0.1 km s^{-1} in the upper and lower crust and lower than 0.05 km s^{-1} in the major part of the upper mantle (Figure 5c).

[15] The results of tomographic inversion may depend on the structure of the reference model. In our case the reference model turned out to be representative of the westernmost section of the seismic profile. To examine the robustness of the results, we chose a reference or starting model that was characterized by velocities reduced relative to the first starting model. With respect to the first approach, this model contained reduced velocities of −4% in the crustal layer and −7% just below Moho in the upper mantle. The RMS travel time misfit using this starting model is 160 ms (χ^2 = 7.66), and for the final model (after five iterations) (Figure 6) it is 50 ms (χ^2 = 1.01). The velocities seaward of the outer rise region were considerably increased already after the first iteration and yielded after five iterations average crustal and upper mantle values. The reduced velocities given in the starting model retained their values in the vicinity of the trench, where the plate is highly affected by the bending stresses. The similarity between this result and our final model confirms the robustness of the resolved features.

[16] Additionally, a series of resolution tests was conducted in order to assess the resolving power of our data set. Synthetic models are constructed using the final velocity model with and without ±5% Gaussian anomalies of different sizes placed at various depths (Figure 7a). Synthetic noise with RMS amplitude of 0.05 s is added to the synthetic travel times obtained from the perturbed velocity model to simulate the addition of actual travel time variation. Both data sets, with and without perturbations, were inverted using the same inversion parameters as the actual model inversions. In the end, the inverted model without perturbations was subtracted from the inverted model with perturbations to yield the final output. After 3 iterations a good resolution was obtained. The velocity anomalies are reasonably well recovered, both in size and amplitude. The ray coverage of our data set is sufficient to resolve features in the uppermost mantle up to ∼4 km below Moho, indicating that a region of reduced velocities within the upper mantle can be resolved. The total depth extent of that anomaly, however, could not be sampled. Owing to the high density of *Pg* rays, the reconstructed anomalies within the crust are remarkably well resolved with the same lateral extent as the original ones (Figure 7b). The weaker amplitude and vertical and lateral smearings of some of the anomalies in the upper mantle and at the Moho are related to the lower ray coverage at these depths. The degree of recovery is also sensitive to the model parameters used to conduct the inversion.

6. Discussion

[17] Application of the seismic tomography method to the Middle America subduction zone, offshore of Nicaragua, reveals new structural details within the subducting oceanic slab. The most significant feature of the tomographic image is an extensive zone of reduced velocities in the crust and upper mantle in the near-trench region, indicating changes of the physical properties consistent with hydration of the subducting oceanic slab, produced after fracturing caused by bending of the subducting slab and perhaps percolation of seawater along the outer rise faults. The systematic change from normal oceanic crust seaward of the outer rise toward reduced velocities in crust and upper mantle indicates that we are observing an evolutionary process. Previous data sets failed to show this characteristic [*Grevemeyer et al.*, 2007].

[18] A detailed study of the relationship between bending-related faulting at trenches and intermediate-depth seismicity along segments of Middle America and Chile trenches shows that the distribution of nodal planes of the intermediate-depth events are remarkably similar to the orientation and dip of the bend faults, for each segment of the study area, and therefore supports the model where the outer rise

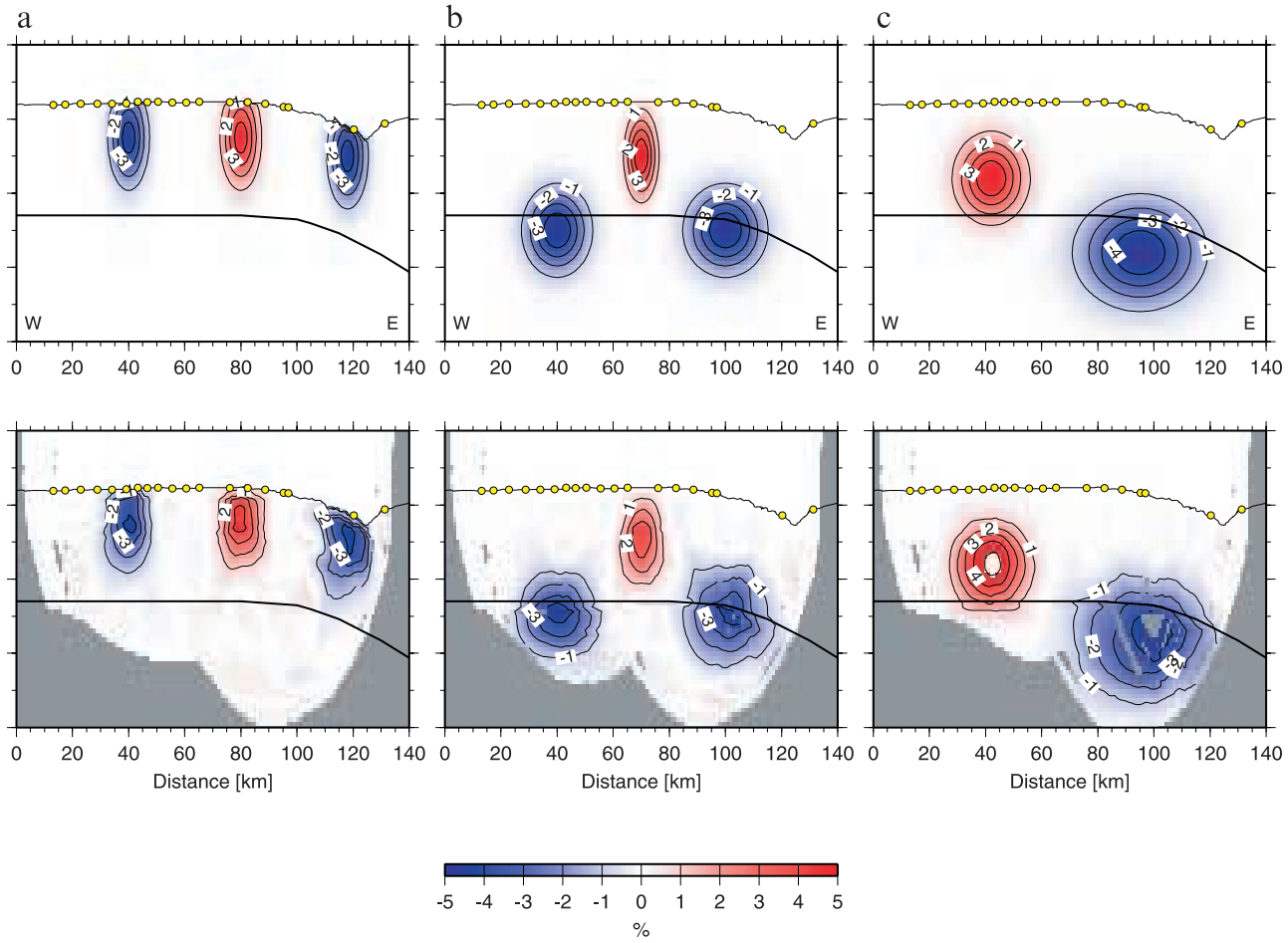

Figure 7. Results of the resolution tests for (a) crustal and (b–c) near Moho depths. Velocity anomalies of −5% to 5% in the synthetic models are given with respect to the final velocity model (Figure 4a).

faults are reactivated at depth [*Ranero et al.*, 2005]. The depth down to which the faults cut into the crust or mantle is poorly known, because the centroid depth of earthquakes is difficult to determine for shallow events occurring below the oceans [e.g., *Yoshida et al.*, 1992], though detailed waveform inspection of Central American trench-outer rise earthquakes suggests that events of M > 6 cut ∼15 km into the mantle [*Lefeldt and Grevemeyer*, 2008]. That coincides with the multichannel seismic reflection images acquired offshore of Nicaragua, which show a pervasive set of trenchward dipping features that cross the crust and extend into the mantle to depths of ∼20 km below the seafloor [*Ranero et al.*, 2003]. Additionally, the same images show that the number of faults and their offsets increase toward the trench axis, which is in agreement with our model, where we find an increase in amplitude and extent of the velocity anomalies as one approaches from the outer rise to the trench. Heat flow data from the Nicaragua trench suggest that faulting of the trench-ocean slope reactivates a vigorous hydrothermal circulation system in the incoming plate. Heat flow decreases toward the trench and hence indicates that seawater mines heat [*Grevemeyer et al.*, 2005]. Interfingering between an upper crustal hydrothermal circulation system and faults cutting down to mantle depth may facilitate migration of seawater along the fault to reach and hydrate the uppermost mantle.

[19] Reduced crustal velocities at the trench can be explained by both hydrothermal alteration and the effect of crustal cracks and fissures on seismic velocity. An increase in fracture porosity just by a few percent may have a significant impact on the seismic velocity structure of the crust. The *Kuster and Toksöz* [1974] model for cracks with varying pore geometry was used by *Wilkens et al.* [1991] to study the evolutionary effect of hydrothermal circulation through the flanks of mid-ocean ridge on the seismic properties of the crust. They have investigated basalt velocity-porosity relationships for a wide range of pore sizes. Their efforts concentrated on how seismic velocities can change by the presence of cracks. Their model suggested a pore space modification with crustal age, where low aspect ratio pore spaces (small and thin cracks) are bridged first and then large aspect ratio voids (wider cracks). In this way seismic velocities can easily be increased with a small reduction of effective porosity, because of the control that thin cracks have on velocity. It is likely that plate bending increases the fracture porosity. Because of the geometry of normal faults, it might be reasonable to hypothesize that bending causes low aspect ratio cracks in crust and mantle. Small changes in fracture

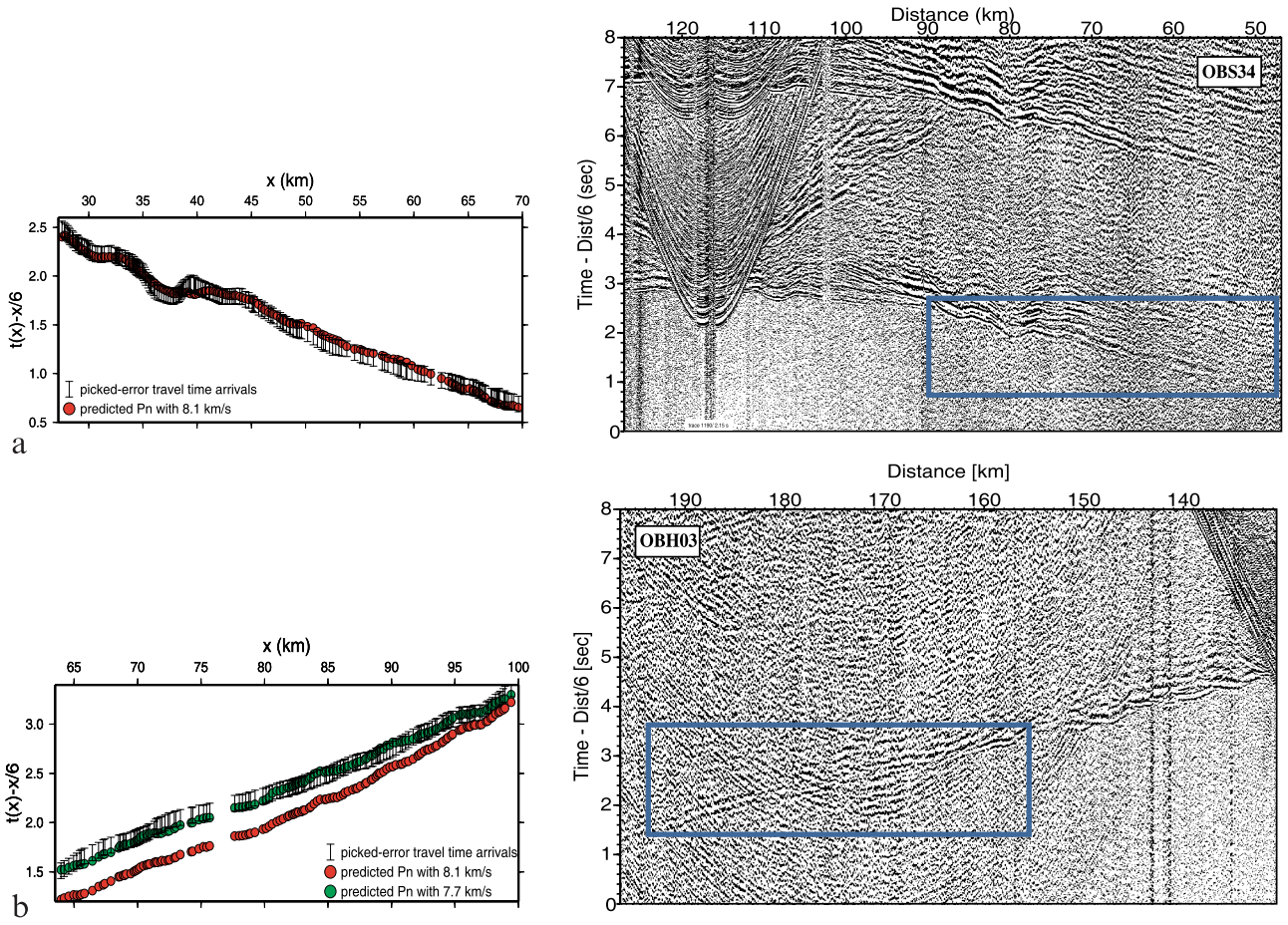

Figure 8. Detailed forward analysis of *Pn* travel times. (a) Trenchward branch of seismic record section of OBS34. (b) Oceanward branch of seismic record section of OBH03.

porosity may therefore explain reduced velocities. However, open cracks and faults in the crust will certainly facilitate fluid migration. Both mechanisms, fracturing and hydration, are therefore related to each other and it might be difficult to separate their effects on seismic properties.

[20] The water content of the lower oceanic crust is, therefore, difficult to constrain. Some estimates have been made for chemically bound water based on the modal mineralogy and seismic properties of oceanic diabase and gabbro samples [*Carlson*, 2003; *Carlson and Miller*, 2004]. Their analysis shows that the H_2O content of diabase dike rocks ranges from 1 to 3%, with an average of 1.5%; gabbros that have velocities typical of the lower oceanic crust (6.7–7.0 km s^{-1}) contain 0.2 to 0.7% H_2O, with a mean near 0.5%.

[21] Anomalously low velocities of the uppermost mantle rocks of 7.6–7.8 km s^{-1} (Figure 8) reveal extensive alteration due to percolation of seawater and serpentinization of mantle peridotite. On the basis of the model developed by *Carlson and Miller* [2003] that relates the degree of serpentinization and water content of partially serpentinized peridotites to their seismic *P* wave velocities, we estimate that the water stored in this region may range from 1.55 to 2.17 wt %, corresponding to a 12–17% increase in serpentine content. Considering the effects of fracture porosity, this number is an upper bound on the water content of a hydrated mantle.

[22] Offshore of south central Chile, *P* wave velocity of the subducting uppermost mantle is found to be reduced to ~7.8 km s^{-1} (~9% serpentinization) [*Contreras-Reyes et al.*, 2007]. The lower anomaly here, compared to the estimates for our study area, or for the Nazca plate at the north Chile trench (~17% serpentinization) [*Ranero and Sallarès*, 2004], is most likely due to the much thicker sediment cover (~2 km). *Contreras-Reyes et al.* [2007] speculate that hydration in a sedimented trench is caused by fluid inflow through basement outcrops, like seamounts, in the outer rise area that penetrate the thick sediment blanket. However, the water/rock ratio will be much lower and hence we would expect a lower degree of hydration.

[23] A high water content in the subducting lithosphere off Nicaragua is consistent with the measurements of water concentration in olivine-hosted melt inclusions along the Central American arc. *Roggensack et al.* [1997] have found very high water concentrations in mafic melt inclusions at Cerro Negro Volcano in Nicaragua (>6 wt %), the highest in any basaltic liquid on the planet. Central American arc volcanism shows strong regional trends in lava chemistry, which reflects different slab contributions to arc melting. The Nicaraguan volcanic arc has one of the highest concentrations of geochemical tracers for oceanic crustal fluid (e.g., boron). It has been proposed that the stronger slab signal in Nicaraguan, compared to Costa Rican arc lavas, reflects greater amounts of fluid released from the dehydra-

tion of a more extensively serpentinized slab mantle [*Rüpke et al.*, 2002]. It should be noted that the Nicaraguan slab, relative to the other Pacific slabs, enters the trench at a very steep angle, which might induce deeper fracture in the slab to account for the high fluid fluxes from the oceanic crust [*Kirby*, 1995; *Patino et al.*, 2000].

7. Conclusions

[24] A tomographic joint inversion of seismic refraction and wide-angle reflection data collected offshore of Nicaragua yields anomalously low seismic *P* wave velocities in the crust and uppermost mantle of the subducting Cocos plate. Seismic velocities of the subducting lithosphere change systematically from seaward of the outer rise toward the trench, indicating an evolutionary process.

[25] Seaward of the outer rise, where the plate is still not affected by the bending stresses, velocities in the crust and upper mantle are typical for mature unaltered oceanic lithosphere. However, as the plate approaches the trench, velocities decrease and the low-anomaly zone increases both in extent and amplitude. This velocity trend coincides with the multichannel seismic reflection (MCS) data acquired offshore of Nicaragua, which shows an increase in the number of bending-related normal faults and their offsets toward the trench axis.

[26] Reduced crustal and upper mantle velocities at the trench are most likely caused by both hydrothermal alteration and an increase in fracture porosity.

[27] In the vicinity of the trench axis upper mantle velocities are in the range 7.6–7.8 km^{-1}, which is 5–7% lower than the ~8.1–8.2 km^{-1} found seaward of the outer rise. The impact of the fractures on the velocity structure could be significant, but difficult to constrain. Thus, an estimate of 12–17% increase in serpentine content in the uppermost 3–4 km of the mantle represents only an upper bound on the degree of hydration.

[28] The anomalously low-velocity zone within the Cocos oceanic lithosphere at the trench offshore of Nicaragua supports the idea that pervasive bending-related normal faulting of a subducting slab creates pathways for seawater to reach and react with cold mantle rocks producing serpentine, implying that deep and widespread hydration (serpentinization) of incoming lithosphere can occur when lithosphere is strongly faulted; thus, the subduction water cycle is closely related to the crustal structure and hydration of the incoming plate.

[29] **Acknowledgments.** We are grateful to the master, officers, and crew of R/V *Sonne* cruise 173 for their cooperation. We thank Greg Moore, Dale Sawyer, and one anonymous reviewer for a number of useful comments and suggestions that improved the presentation of our results. This study was funded by the German Ministry for Education, Science and Technology (R/V *Sonne* cruises SO173-1 and SO173-2) and the German Science foundation (DFG) through the SFB 574 "Volatiles and fluids in subduction zones" at Christan-Albrechts University, Kiel. SFB 574 contribution 132.

References

Berhorst, A. (2006), Die Struktur des aktiven Kontinentalrands vor Nicaragua und Costa Rica - marin-seismische Steil- und Weitwinkelmessungen, Dissertation, 159 pp., Christian Albrechts Univ., Kiel.

Bialas, J., and E. R. Flueh (1999), Ocean bottom seismometers, *Sea Technol.*, *40*(4), 41–46.

Burbach, G. V., C. Frolhich, W. D. Pennington, and T. Matumoto (1984), Seismicity and tectonics of the subducted Cocos plate, *J. Geophys. Res.*, *89*, 7719–7735, doi:10.1029/JB089iB09p07719.

Carlson, R. L. (1998), Seismic velocities in the uppermost oceanic crust: Age dependence and the fate of layer 2A, *J. Geophys. Res.*, *103*, 7069–7077, doi:10.1029/97JB03577.

Carlson, R. L. (2003), Bound water content of the lower oceanic crust estimated from modal analyses and seismic velocities of oceanic diabase and gabbro, *Geophys. Res. Lett.*, *30*(22), 2142, doi:10.1029/2003GL018213.

Carlson, R. L., and D. J. Miller (2003), Mantle wedge water contents estimated from seismic velocities in partially serpentinized peridotites, *Geophys. Res. Lett.*, *30*(5), 1250, doi:10.1029/2002GL016600.

Carlson, R. L., and D. J. Miller (2004), Influence of pressure and mineralogy on seismic velocities in oceanic gabbros: Implications for the composition and state of the lower oceanic crust, *J. Geophys. Res.*, *109*, B09205, doi:10.1029/2003JB002699.

Chapple, W. M., and D. W. Forsyth (1979), Earthquakes and bending of plates at trenches, *J. Geophys. Res.*, *84*, 6729–6749, doi:10.1029/JB084iB12p06729.

Christensen, D. H., and L. J. Ruff (1983), Outer rise earthquakes and seismic coupling, *Geophys. Res. Lett.*, *10*(8), 697–700, doi:10.1029/GL010i008p00697.

Christensen, D. H., and L. J. Ruff (1988), Seismic coupling and outer rise earthquakes, *J. Geophys. Res.*, *93*, 13,421–13,444, doi:10.1029/JB093iB11p13421.

Collins, J. A., G. M. Purdy, and T. M. Brocher (1989), Seismic velocity structure at Deep Sea Drilling Project Hole 504B, Panama Basin: evidence for thin crust, *J. Geophys. Res.*, *94*, 9283–9302, doi:10.1029/JB094iB07p09283.

Contreras-Reyes, E., I. Grevemeyer, E. R. Flueh, M. Scherwath, and M. Heesemann (2007), Alteration of the subducting oceanic lithosphere at the southern central Chile trench-outer rise, *Geochem. Geophys. Geosyst.*, *8*, Q07003, doi:10.1029/2007GC001632.

DeMets, C., R. G. Gordon, D. F. Argus, and S. Stein (1990), Current plate motions, *Geophys. J. Int.*, *101*, 425–478, doi:10.1111/j.1365-246X.1990.tb06579.x.

Dmowska, R., G. Zheng, and J. R. Rice (1996), Seismicity and deformation at convergent margins due to heterogeneous coupling, *J. Geophys. Res.*, *101*, 3015–3029, doi:10.1029/95JB03122.

Fisher, A. T., C. A. Stein, R. N. Harris, K. Wang, E. A. Silver, M. Pfender, M. Hutnak, A. Cherkaoui, R. Bodzin, and H. Villinger (2003), Abrupt thermal transition reveals hydrothermal boundary and role of seamounts within the Cocos plate, *Geophys. Res. Lett.*, *30*(11), 1550, doi:10.1029/2002GL016766.

Flueh, E. R., and J. Bialas (1996), A digital, high data capacity ocean bottom recorder for seismic investigations, *Int. Underwater Syst. Design*, *18*(3), 18–20.

Grevemeyer, I., and A. Bartetzko (2004), Hydrothermal ageing of oceanic crust: inferences from seismic refraction and bore hole studies, in *Hydrogeology of Oceanic Lithosphere*, edited by E. E. Davis and H. Elderfield, pp. 128–150, Cambridge Univ. Press, New York.

Grevemeyer, I., W. Weigel, R. B. Whitmarsh, F. Avedik, and G. A. Dehghani (1997), The Aegir Rift: Crustal structure of an extinct spreading axis, *Mar. Geophys. Res.*, *19*, 1–23, doi:10.1023/A:1004288815129.

Grevemeyer, I., W. Weigel, and C. Jennrich (1998), Structure and ageing of oceanic crust at 14°S on the East Pacific Rise, *Geophys. J. Int.*, *135*, 573–584, doi:10.1046/j.1365-246X.1998.00673.x.

Grevemeyer, I., N. Kaul, H. Villinger, and W. Weigel (1999), Hydrothermal activity and the evolution of the seismic properties of upper oceanic crust, *J. Geophys. Res.*, *104*, 5069–5079, doi:10.1029/1998JB900096.

Grevemeyer, I., N. Kaul, J. L. Diaz-Naveas, H. Villinger, C. R. Ranero, and C. Reichert (2005), Heat flow and bending-related faulting at subduction trenches: case studies offshore of Nicaragua and central Chile, *Earth Planet. Sci. Lett.*, *236*, 238–248, doi:10.1016/j.epsl.2005.04.048.

Grevemeyer, I., C. R. Ranero, E. R. Flueh, D. Kläschen, and J. Bialas (2007), Passive and active seismological study of bending-related faulting and mantle serpentinization at the Middle America Trench, *Earth Planet. Sci. Lett.*, *258*, 528–542, doi:10.1016/j.epsl.2007.04.013.

Hasegawa, A., S. Horiuchi, and N. Umino (1994), Seismic structure of the northeastern Japan convergent margin: A synthesis, *J. Geophys. Res.*, *99*, 22,295–22,312, doi:10.1029/93JB02797.

Jarrard, R. D. (2003), Subduction fluxes of water, carbon dioxide, chlorine, and potassium, *Geochem. Geophys. Geosyst.*, *4*(5), 8905, doi:10.1029/2002GC000392.

Kanamori, H. (1971), Seismological evidence for lithospheric normal faulting—The Sanriku earthquake of 1933, *Phys. Earth Planet. Inter.*, *4*, 289–300, doi:10.1016/0031-9201(71)90013-6.

Kirby, S. H. (1995), Intraslab earthquakes and phase changes in subducting lithosphere, *Rev. Geophys.*, *33*, 287–297, doi:10.1029/95RG00353.

Kobayashi, K., M. Nakanishi, K. Tamaki, and Y. Ogawa (1998), Outer slope faulting associated with western Kuril and Japan trenches, *Geophys. J. Int.*, *134*, 356–372, doi:10.1046/j.1365-246x.1998.00569.x.

Korenaga, J., W. S. Holbrook, G. M. Kent, P. B. Kelemen, R. S. Detrick, H.-C. Larsen, J. R. Hooper, and T. Dahl-Jensen (2000), Crustal structure of the southeast Greenland margin from joint refraction and reflection seismic tomography, *J. Geophys. Res.*, *105*, 21,591–21,614, doi:10.1029/2000JB900188.

Kuster, G. T., and M. N. Toksöz (1974), Velocity and attenuation of seismic waves in two-phase media: part I - Theoretical formulations, *Geophysics*, *39*, 587–606, doi:10.1190/1.1440450.

Lefeldt, M., and I. Grevemeyer (2008), Centroid depth and mechanism of trench-outer rise earthquakes, *Geophys. J. Int.*, *172*(1), 240–251, doi:10.1111/j.1365-246X.2007.03616.x.

Masson, D. G. (1991), Fault patterns at outer trench walls, *Mar. Geophys. Res.*, *13*, 209–225, doi:10.1007/BF00369150.

Meade, C., and R. Jeanloz (1991), Deep-focus earthquakes and recycling of water into the Earth's mantle, *Science*, *252*, 68–72, doi:10.1126/science.252.5002.68.

Moser, T. J. (1991), Shortest path calculation of seismic rays, *Geophysics*, *56*, 59–67, doi:10.1190/1.1442958.

Moser, T. J., G. Nolet, and R. Snieder (1992), Ray bending revisited, *Bull. Seismol. Soc. Am.*, *82*, 259–288.

Osler, J. C., and K. E. Louden (1995), Extinct spreading center in the Labrador Sea: Crustal structure from a two-dimensional seismic refraction velocity model, *J. Geophys. Res.*, *100*, 2261–2278, doi:10.1029/94JB02890.

Paige, C. C., and M. A. Saunders (1982), LSQR: An algorithm for sparse linear equations and sparse least squares, *ACM Trans. Math. Software*, *8*, 43–71, doi:10.1145/355984.355989.

Patino, L. C., M. J. Carr, and M. D. Feigenson (2000), Local and regional variations in Central American arc lavas controlled by variations in subducted sediment input, *Contrib. Mineral. Petrol.*, *138*, 265–283, doi:10.1007/s004100050562.

Peacock, S. M. (2001), Are the lower planes of double seismic zones caused by serpentine dehydration in subducting oceanic mantle?, *Geology*, *29*, 299–302, doi:10.1130/0091-7613(2001)029<0299:ATLPOD>2.0.CO;2.

Peacock, S. M. (2004), Insight into the hydrogeology and alteration of oceanic lithosphere based on subduction zones and arc volcanisms, in *Hydrogeology of Oceanic Lithosphere*, edited by E. E. Davis and H. Elderfield, pp. 659–676, Cambridge Univ. Press, New York.

Phipps Morgan, J. (2001), The role of serpentinization and deserpentinization in bending and unbending the subducting slab, *Eos Trans. AGU*, *82*(47), Fall Meet. Suppl., Abstract T22D-03.

Protti, M., F. Güendel, and K. McNally (1994), The geometry of the Wadati-Benioff zone under southern Central America and its tectonic significance: results from a high-resolution local seismographic network, *Phys. Earth Planet. Inter.*, *84*, 271–287, doi:10.1016/0031-9201(94)90046-9.

Raleigh, C. B., and M. S. Paterson (1965), Experimental deformation of serpentinite and its tectonic implications, *J. Geophys. Res.*, *70*, 3965–3985, doi:10.1029/JZ070i016p03965.

Ranero, C. R., and V. Sallarès (2004), Geophysical evidence for alteration of the crust and mantle of the Nazca Plate during bending at the north Chile trench, *Geology*, *32*, 549–552, doi:10.1130/G20379.1.

Ranero, C. R., J. Phipps Morgan, K. McIntosh, and C. Reichert (2003), Bending, faulting, and mantle serpentinization at the Middle America Trench, *Nature*, *425*, 367–373, doi:10.1038/nature01961.

Ranero, C. R., A. Villaseñor, J. Phipps Morgan, and W. Weinrebe (2005), Relationship between bend-faulting at trenches and intermediate-depth seismicity, *Geochem. Geophys. Geosyst.*, *6*, Q12002, doi:10.1029/2005GC000997.

Roggensack, K., R. L. Hervig, S. B. McKnight, and S. N. Williams (1997), Explosive basaltic volcanism from Cerro Negro volcano: Influence of volatiles on eruptive style, *Science*, *277*, 1639–1642, doi:10.1126/science.277.5332.1639.

Rüpke, L., J. Phipps Morgan, M. Hort, and J. A. D. Connoly (2002), Are the regional variations in Central American arc lavas due to differing basaltic peridotitic slab sources of fluids?, *Geology*, *30*, 1035–1038, doi:10.1130/0091-7613(2002)030<1035:ATRVIC>2.0.CO;2.

Staudigel, H., T. Plank, W. M. White, and H. Schmincke (1996), Geochemical fluxes during seafloor alteration of the upper oceanic crust: DSDP sites 417 and 418, in *Subduction From Top to Bottom, Geophys. Monogr. Ser.*, vol. 96, edited by G. E. Bebout et al., pp. 19–38, AGU, Washington, D. C.

Tarantola, A. (1987), *Inverse Problem Theory: Methods for Data Fitting and Model Parameter Estimation*, 613 pp., Elsevier, New York.

Toomey, D. R., and G. R. Foulger (1989), Tomographic inversion of local earthquake data from the Hengill-Grensdalur central volcano complex, Iceland, *J. Geophys. Res.*, *94*, 17,497–17,510, doi:10.1029/JB094iB12p17497.

von Huene, R., C. R. Ranero, W. Weinrebe, and K. Hinz (2000), Quaternary convergent margin tectonics of Costa Rica, segmentation of the Cocos plate, and Central American volcanism, *Tectonics*, *19*, 314–334, doi:10.1029/1999TC001143.

Walther, C. H. E., E. R. Flueh, C. R. Ranero, R. von Huene, and W. Strauch (2000), Crustal structure across the Pacific margin of Nicaragua: evidence for ophiolitic basement and a shallow mantle sliver, *Geophys. J. Int.*, *141*, 759–777, doi:10.1046/j.1365-246x.2000.00134.x.

White, R. S., D. McKenzie, and R. K. O'Nions (1992), Oceanic crustal thickness from seismic measurements and rare earth element inversions, *J. Geophys. Res.*, *97*, 19,683–19,715, doi:10.1029/92JB01749.

Wilkens, R. H., G. J. Fryer, and J. Karsten (1991), Evolution of porosity and seismic structure of upper oceanic crust: Importance of aspect ratios, *J. Geophys. Res.*, *96*, 17,981–17,995, doi:10.1029/91JB01454.

Wilson, D. S., et al. (2003), *Proceedings of the Ocean Drilling Program, Initial Reports*, vol. 206, Ocean Drill. Program, College Station, Tex., doi:10.2973/odp.proc.ir.206.2003.

Yoshida, Y., K. Satake, and K. Abe (1992), The large normal-faulting Mariana earthquake of April 5, 1990 in uncoupled subduction zone, *Geophys. Res. Lett.*, *19*, 297–300, doi:10.1029/92GL00165.

Zhang, J., and M. N. Toksöz (1998), Nonlinear refraction traveltime tomography, *Geophysics*, *63*, 1726–1737, doi:10.1190/1.1444468.

A. Berhorst, E. R. Flueh, and I. Grevemeyer, Leibniz Institut fuer Meereswissenschaften, IFM-GEOMAR, Wischhofstrasse 1-3, D-24148 Kiel, Germany. (igrevemeyer@ifm-geomar.de)

M. Ivandic, Sonderforschungsbereicht 574, Wischhofstrasse 1-3, D-24148 Kiel, Germany. (mivandic@ifm-geomar.de)

K. McIntosh, Institute for Geophysics, University of Texas at Austin, 10100 Burnet Road, R2200, Pickle Research Campus, ROC, Austin, TX 78758-4445, USA.